Void fraction thermo-kinematics for subcooled flow boiling

Cite as: Phys. Fluids **34**, 123302 (2022); https://doi.org/10.1063/5.0120149
Submitted: 11 August 2022 • Accepted: 10 November 2022 • Published Online: 01 December 2022

F. J. Collado

Physics of Fluids ARTICLE scitation.org/journal/phf

Void fraction thermo-kinematics for subcooled flow boiling

Cite as: Phys. Fluids **34**, 123302 (2022); doi: 10.1063/5.0120149
Submitted: 11 August 2022 · Accepted: 10 November 2022 ·
Published Online: 1 December 2022

F. J. Collado[a)]

AFFILIATIONS

Department of Mechanical Engineering, Universidad de Zaragoza, Zaragoza 50018, Spain

Note: This paper is part of the special topic, Multiphase flow in energy studies and applications: A special issue for MTCUE-2022.
[a)]**Author to whom correspondence should be addressed:** fjk@unizar.es

ABSTRACT

This work presents some preliminary results about a new void fraction model in subcooled flow boiling based on brand new mass and energy balances developed by the author over the past years. As main novelties, the new mass balance is based on the liquid velocity and the mixture specific volume, whereas the new heat balance is a function of the mixture enthalpy, based on the thermodynamic quality, and explicitly includes the mean vapor–liquid velocity ratio, or the slip ratio. The core of the model is to predict the slip ratio profile and then to calculate the mixture enthalpy from the new heat balance and, finally, to derive the void fraction. In this work, it is shown that the continuity of the first derivative of the mixture specific volume just at saturation establishes a first equation to obtain the slip evolution. A second kinematic equation between the onset of nuclear boiling (ONB) and the vapor velocity is also found. Three additional parameters, related to the ONB and the point of net vapor generation, are needed for void fraction profiles predictions, which have been found by trial and error, searching the best fitting to the measured void fraction. The new model is compared to eight full axial void fraction profiles data for upward subcooled flow of water at high pressure.

NOMENCLATURE

A	Cross-sectional area of the tube (m^2)
D	Tube diameter (m)
G	Mass flux (kg/m^2s)
h	Specific enthalpy (J/kg)
p	Pressure (Pa)
q	Specific heat per unit length (J/mkg)
q''	Heat flux (W/m^2)
S	Mean vapor–liquid velocity ratio or slip ratio (-)
T	Temperature (K)
u	Cross-sectional average velocity (m/s)
v	Specific volume (m^3/kg)
W	Mass flow rate (kg/s)
x	"Static" or "Thermodynamic" quality (-)
x_e	"Equilibrium" quality (-)
x_d	"Flow quality" or mass dryness fraction (-)
z	Tube axis direction (m)

Special characters

α	Vapor void fraction (-)
β	Volumetric coefficient of thermal expansion (p const.) (1/K)
ρ	Density (kg/m^3)

Subscripts

F	Saturated liquid
G	Saturated vapor
i	Inlet
L	Subcooled liquid
m	Liquid-saturated vapor mixture
NVG	(Point of) Net vapor generation
ONB	Onset of Nuclear Boiling
sat	Saturated
0	Partially subcooled boiling region
1	Fully subcooled boiling region
2	Saturated boiling region

INTRODUCTION

Modeling of subcooled flow boiling, i.e., the flow of the subcooled liquid through a heated channel in which a net amount of saturated vapor (bubbles) is produced, is of utmost importance for a huge

variety of industrial systems.[1,2] One of the major parameters characterizing such liquid-vapor flows is the void fraction, α, representing the fraction of the channel cross-sectional area occupied by the gas or vapor phase.

Figure 1 shows that the subcooled flow zone starts at the onset of nucleate boiling (ONB), when the wall temperature is around a saturation one and goes right up to the point where the liquid reaches saturation and bulk boiling commences.

The subcooled zone is divided into two regions, i.e., "partially subcooled" and "fully subcooled" regions.[1,2] The partially subcooled region initiates at the ONB point, where bubbles start to be generated on the heated surface of the tube. However, the bubbles do not grow further because of rapid condensation with the surrounding subcooled liquid. Thus, given the low void fractions ($\alpha < 4-5\%$), this zone is usually neglected in the empirical void models.[3] In the fully subcooled region, α increases rapidly from the point of net vapor generation (NVG), which is also called the onset of significant void fraction (OSV).

Recently, following an exhaustive comparison of available void fraction datasets with 49 models and correlations for α published since 1959 until 2021, Mudawar and co-workers[3] affirm that, due to the complexity in treating thermodynamic (and kinematic) non-equilibrium effects in subcooled flows, predicting the void fraction in a purely theoretical manner is a formidable challenge. This is why most published α relations follow empirical formulations. In conclusion, a robust and accurate method to predicting the void fraction is still lacking and, therefore, warrants a careful further study.[3]

Standard one-dimensional void fraction models

Standard one-dimensional (1D) bubbly flow models start from classic averaged 1d conservation equations of mass and energy for a two-phase flow. However, the aforementioned lack of thermodynamic and kinematic equilibrium between the vapor and liquid phases confuses the mass and energy balances, so up to three different qualities are considered in Ref. 4; in particular, the equilibrium quality, x_e, the flow quality, x_d, and the so-called static quality, x. In this work, the latter is considered the actual mass fraction of vapor, i.e., the actual thermodynamic quality.

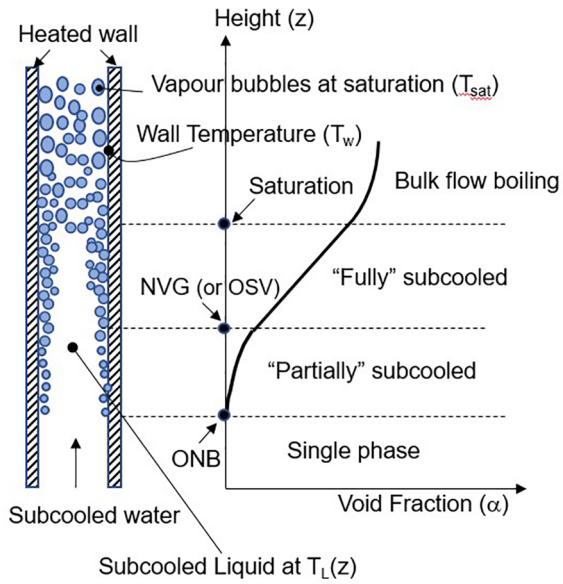

FIG. 1. ONB and NVG locations in subcooled flow boiling.

The equilibrium quality x_e is derived from the standard energy balance,[3,4] then, for a uniformly heated circular tube, it is defined as

$$x_e = \frac{h_L(z) - h_F}{\Delta h_{FG}} = \frac{\frac{4q''z}{GD} + h_{Li} - h_F}{\Delta h_{FG}} = \frac{qz + h_{Li} - h_F}{\Delta h_{FG}}, \quad (1)$$

where $h_L(z)$ is calculated with the classical single flow heat balance, and Δh_{FG} is the latent heat of vaporization. Notice that x_e takes negative values in the subcooled regions until reaching saturation.

On the other hand, it is considered[4] that the so-called flow quality, also called mass dryness fraction,[3,4] x_d, is the true flow fraction of vapor. It is based on the standard liquid and vapor mass balances[4] and is defined as the ratio of the mass flow rate of vapor to the total flow rate. That is,

$$x_d = \frac{W_G}{W_G + W_L} = \frac{\rho_G u_G \alpha A}{\rho_G u_G \alpha A + \rho_L u_L (1-\alpha) A}. \quad (2)$$

Similar to the void fraction, x_d ranges from 0 to 1 and would become equivalent to x_e only for bulk flow boiling situations.

Note that the current void fraction correlations[3] are generally expressed as a function of the flow quality x_d, although this quality cannot be directly calculated from Eq. (2). Instead, there have been proposed[3] appropriate (empirical) x_d relations in a function of x_e, Eq. (1), and the equilibrium quality where the NVG point occurs, $x_{e,NVG}$. Following Ref. 3, the most used empirical correlation to obtain $x_d(x_e,\ x_{e,NVG})$ is the Saha and Zuber correlation[5]

$$x_d = \frac{W_G}{W_G + W_L} = \frac{x_e - x_{e,NVG}\ \exp\left(x_e/x_{e,NVG} - 1\right)}{1 - x_{e,NVG}\ \exp\left(x_e/x_{e,NVG} - 1\right)}. \quad (3)$$

Clearly, there is also a necessary correlation for the equilibrium quality at the point of NVG, $x_{e,NVG}$. In Ref. 3, 16 published correlations for this quality are processed.

Finally, the standard predictive methods for the void fraction try to relate α with the flow quality x_d. The most relevant categories are the slip ratio and drift flux models.

The slip ratio procedures combine the standard definitions of the void fraction and mass dryness fraction, yielding the following relation:

$$\alpha = \frac{1}{1 + S\left(\frac{1-x_d}{x_d}\right)\frac{\rho_G}{\rho_L}}, \quad (4)$$

where S is the vapor–liquid velocity ratio, or the slip ratio, given by

$$S = \frac{u_G}{u_L}, \quad (5)$$

and u_G and u_L are the cross-sectional average of the vapor velocity and the cross-sectional average of the liquid velocity, respectively. In terms of the void fraction prediction,[3] the simple slip ratio model of Thom[6] achieves best accuracy.

The drift flux void fraction model, proposed by Zuber and Findlay,[7] is a variation of the slip model substituting the slip ratio by two new parameters

$$\alpha = \frac{x_d}{C\left[1 + \frac{\rho_G}{\rho_L}(1 - x_d)\right] + \frac{\rho_G u_{Gj}}{G}}, \tag{6}$$

where C is termed the "distribution parameter," related to the non-uniformity of the flow profile, and u_{Gj} is the "drift" velocity, or the local relative velocity between the phases. There are tenths[3] of drift flux models, each one with its own C and u_{Gj} expressions. In Ref. 3, the drift flux model of Dix[8] is stood out from the rest.

Conversely, these two parameters are also a function of the different flow patterns (churn turbulent flow, annular flow, bubbly flow, etc.) found along the duct, which is necessary to define in function of the operating conditions.

New void fraction model based on "static" quality

The starting point of the new void fraction model presented here was suggested by the author some years ago, i.e., to work with the well-known static or thermodynamic quality, x, which is the third quality, suggested in Ref. 4, to pose a new heat balance[9–12] from which the void fraction could be derived. x is defined as follows:[4]

$$x = \frac{\alpha\rho_G}{\alpha\rho_G + (1 - \alpha)\rho_L} = \frac{\alpha\rho_G}{\rho_m}, \tag{7}$$

where ρ_m is the vapor (G)–liquid (L) mixture density.

The justification is that such quality does have a direct and strong connection, Eq. (7), with the void fraction.

In order to search a new heat balance based on x, mixture properties based on such quality have been already formulated; [9–12] in particular, the mixture density ρ_m, which is defined in Eq. (7), and the mixture enthalpy, h_m, which is given by

$$h_m = xh_G + (1 - x)h_L. \tag{8}$$

A brand new heat balance, including the above mixture enthalpy, has been already presented elsewhere[9–12]

$$\frac{\frac{4q''z}{GD}}{\Delta h_m} = \frac{qz}{\Delta h_m} \sim S \rightarrow \frac{dh_m}{dz} \sim \frac{q}{S}, \tag{9}$$

where q(kJ/kg m) is the uniform heat per unit inlet mass and per unit length, and Δh_m (kJ/kg) is the mixture enthalpy increment between the inlet and some point located at z (axial distance from the inlet).

Also note that the new heat balance is only one equation with two unknowns, namely, the mixture enthalpy, h_m, which includes the desired void fraction, and the slip ratio, S.

A brand new mass balance,[13] coherent with the above new heat balance,[9–12] would be

$$W_{L,i} = \frac{W_G}{S} + W_L = \frac{\rho_G u_G \alpha A}{u_G/u_L} + \rho_L u_L (1 - \alpha)A = \rho_m u_L A, \tag{10}$$

where $W_{L,i}$ is the subcooled water inlet mass flow rate, whereas W_G and W_L are the vapor and liquid ones, respectively.

In Eqs. (9) and (10), the common time reference is that of the liquid phase, which is the continuous phase, whereas vapor is the dispersed phase.

Point out that phase velocities are usually considered different from each other,[1–4] but as the control volume length (the length of some duct section) is the same for both phases, phase timescales have to be different each other too.

Therefore, the slip ratio would act as a timescale change factor

$$S = \frac{u_G}{u_L} \sim \frac{\Delta z/\Delta t_G}{\Delta z/\Delta t_L} \sim \frac{\Delta t_L}{\Delta t_G}. \tag{11}$$

In Eq. (9), it is assumed that the heat would enter the liquid–vapor mixture through condensing bubbles, i.e., with the vapor time reference, and then, the heat flux is divided by the slip ratio.

These new mass and heat balances have been already checked against accurate void fraction data several times.[9–12] Such comparisons have merely calculated the mixture enthalpy profiles, Eq. (8), which include the void fraction data, Eq. (7), and then, following Eq. (9), derived the corresponding slip ratio profile.

The central objective should be to predict the slip ratio profile along the heated channel exclusively from the operating conditions, since reversing the process, we could calculate the mixture enthalpy from the heat balance and then the void fraction.

For subcooled flow boiling tests measured by Bartolomei *et al.*[14] from Moscow Power Institute (MPI) in 1980s, the author has already published[12] good fittings of the slip ratio profile varying only two key slip ratio values, namely, the slip ratio just at saturation point, $S_{1,sat}$, and a constant slip along the saturation zone, S_2. The location of the point of Net Vapor Generation (NVG)[1–3,5,14] was also varied in the fitting.

Although it was clearly shown[12] that higher the accuracy of the slip ratio prediction, higher the calculated void fraction accuracy, we do not know yet how to calculate the slip ratio profile from the inlet conditions and then to close the new heat balance.

In this work, the options to calculate such key slip ratio values, now based on first principles, in addition to estimating the significant locations as the onset of nuclear boiling (ONB) and the NVG (thus, to predict the void fraction) are explored.

The new void fraction modeling is assessed against eight out of 24 axial void fraction profile tests reported by MPI in Ref. 14 for water entering a vertical uniformly heated tube of 12 mm diameter at high pressure and subcooling. The volumetric steam content α was determined by γ-ray whose maximum absolute error did not exceed ± 4%.[14]

As can be seen in Table I, the selected tests for this work have a wide range of operational conditions of industrial interest.

NEW HEAT BALANCE FUNCTION OF THE SLIP RATIO

To explain the new void fraction model, it is applied in detail to the first test in Table I, the so-called tests 1–3 in Ref. 12.

Figure 2 shows the measured void fractions (circles) in a function of z, which were originally reported in a function of x_e,[14] and the calculated void fraction profile (bold line) proposed in this work and explained later.

From measured $\alpha(z)$ curves, i.e., Fig. 2, the rough ONB and NVG locations could be easily spotted: the ONB should be around the beginning of the voids ($\alpha > 0$), whereas the NVG would be after the ONB and near the bending change of the void curve when an approximately straight line commences. The ONB and NVG fitted locations, in addition to the void fraction at NVG, are shown in Fig. 2. As we will explain later, these three parameters have been found by trial and error to best fitting the model to data.

TABLE I. Operational conditions, fittings, and results for the analyzed void fraction tests.

#	p_i (MPa)	G (kg/m^{2}s)	q'' (MW/m^2)	ΔT_{sub} (°C)	z_{ONB} (m)	z_{NVG} (m)	α_{NVG}	$S_{1,sat}$	S_2
1-3	6.84	961	1.13	91.4	0.6	0.8	0.065	0.7912	2.381
2a-1	6.81	998	0.44	36.1	0.22	0.88	0.015	0.7894	2.423
2a-5	7.01	996	1.98	125	0.45	0.72	0.17	0.8241	3.071
3a-1	6.89	405	0.79	137	0.6	0.72	0.1	0.799	2.47
3b-1	11.02	503	0.99	97.4	0.38	0.52	0.1	0.7864	1.961
3b-2	10.81	966	1.13	87.9	0.64	0.83	0.06	0.7626	1.823
3b-3	10.81	1554	1.16	26.9	0.02	0.02	0.025	0.8142	1.632
3b-4	10.84	1959	1.13	27.1	0.23	0.40	0.01	0.7485	1.494

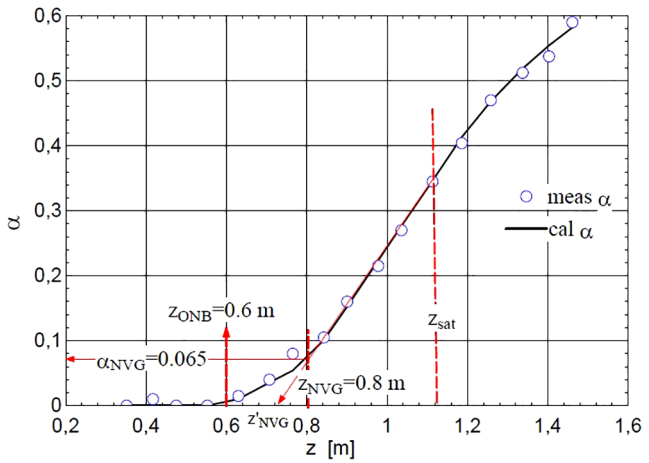

FIG. 2. Void fraction profile α for tests 1–3.

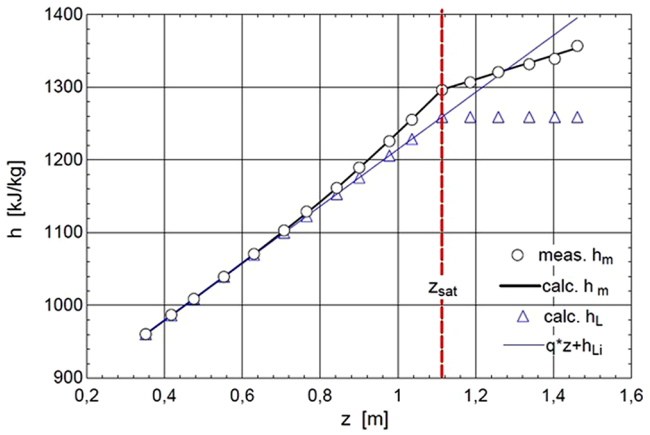

FIG. 3. Mixture enthalpy profile h_m for tests 1–3.

Data reduction

The model begins by plotting the corresponding mixture enthalpy axial profile (circles), see Fig. 3, based on the measured void fraction (Fig. 2). Notice that, under uniform heat flux, there is a strong discontinuity of the enthalpy slope in reaching saturation. The details of such enthalpy calculation, which are based on Eqs. (7) and (8), are as follows.

First, we assume a constant pressure along the channel equal to the inlet pressure. This assumption is also implicitly included in the standard models, when calculating x_e, which is a function of the liquid and vapor saturated enthalpies corresponding to the reference test pressure, see the solved examples in Ref. 1, and also in the slip ratio and drift flux models, which work with only one pressure data.[3]

For the liquid enthalpy along the subcooled region in Eq. (8), $h_L(z)$, the standard approach[1,2] of considering practically equal to the "flow" mixture enthalpy is assumed:

$$h_L(z) \approx qz + h_{L,i} \rightarrow h_F = qz_{sat} + h_{L,i}, \tag{12}$$

where $h_{L,i}$ is the subcooled liquid enthalpy at the input conditions, and h_F is the saturated liquid enthalpy. Then, the axial location of the saturation point, z_{sat}, can be easily calculated.

Saturation properties of the liquid and vapor have been read in thermodynamic tables entering with inlet pressure. On the other hand, the subcooled liquid density, necessary in Eq. (7), have been also read in tables with the pressure and the above liquid enthalpy, Eq. (12).

Finally, from Eq. (7), the quality is obtained, and then, from Eq. (8), the "measured" mixture enthalpy, see the circles in Fig. 3.

Next, the S profile for tests 1–3 could be derived from the new heat balance, Eq. (9), relating the mixture enthalpy increment along a tube interval with the heat applied and the interval length.

In this proposal, at difference from preliminary works[12] and following the standard procedures,[3] the flow boiling is divided into four zones, see Fig. 3. The first one, at the beginning of the tube, is the subcooled liquid only or a single flow, in which the standard heat balance, Eq. (12), works. As there is no vapor, S is technically not defined. However, S is set to 1 by convention and also searching coherence between Eqs. (9) and (12).

As we have already commented above, the partially subcooled boiling zone starts at the ONB and finishes at the NVG. Finally, the fully subcooled zone ends when the liquid reaches saturation. Hence, we should analyze the slip ratio evolution along the last three zones.

Slip ratio in the partially subcooled flow boiling zone, S_0

For the partially subcooled flow boiling zone, i.e., from the ONB until the NVG, see Fig. 3, the slip ratio in this region, denoted by S_0,

is derived from the void fraction measurements, which supply the mixture enthalpy, through a modified expression of the new heat balance, Eq. (9),

$$h_m(z) = \frac{q}{S_0(z)}(z - z_{ONB}) + h_{L,ONB} \rightarrow S_0(z) \approx \frac{q(z - z_{ONB})}{h_m(z) - h_{L,ONB}}. \quad (13)$$

Note that following the standard procedures,[1–3] it is assumed that there is liquid only at z_{ONB}. After the ONB point, there is a steady, although rather slow, growth of the steam content in flow boiling. Therefore, the corresponding slip ratio should be set to a value lower than 1, so that the mixture enthalpy was greater than the liquid enthalpy alone.

In Eq. (13), it is clear that the slip ratio calculation actually supplies an average of the local S values from the ONB until the specific axial location z in this zero zone. This averaging mitigates the measure dispersion and eases trend assessment.

As we will see later for the following zone, the reference to establish the averages will be changed from the ONB point to the NVG one. This is an improvement in relation to previous works,[12] in which the average of the local slip values always ranged from the tube inlet ($z = 0$) to a particular location z for the two subcooled flow boiling zones.

Therefore, the last enthalpy of this partially subcooled zone corresponds with that of the NVG point, $h_{m,NVG}$, that is,

$$h_{m,NVG} = \frac{q}{S_0(z_{NVG})}(z_{NVG} - z_{ONB}) + h_{L,ONB}. \quad (14)$$

Logically, to preserve enthalpy continuity, this enthalpy should also be the first value for the following zone, i.e., the fully subcooled one.

Slip ratio in the fully subcooled flow boiling zone, S_1

This zone ranges from the NVG until saturation, see Fig. 3. As we have advanced above, here, the slip ratio $S_1(z)$ is an average of the slip local values from the NVG point until z. As before, it is derived from the new heat balance

$$h_m(z) = \frac{q}{S_1(z)}(z - z_{NVG}) + h_{m,NVG} \rightarrow S_1(z) \approx \frac{q(z - z_{NVG})}{h_m(z) - h_{m,NVG}}. \quad (15)$$

Clearly, after reaching saturation, the new reference for the averages of the slip ratio will be the saturation point (z_{sat}). Now, it is necessary to obtain the mixture enthalpy at saturation, $h_{m,sat}$, which is the last point of this zone and the first value of the next bulk zone

$$h_{m,sat} = \frac{q}{S_1(z_{sat})}(z_{sat} - z_{NVG}) + h_{m,NVG}. \quad (16)$$

Remember that one of the key variables of the model is the slip ratio just at saturation coming from the subcooled flow, which previously has been denoted as $S_{1,sat}$. Here,

$$S_{1,sat} = S_1(z_{sat}). \quad (17)$$

Slip ratio in the bulk (saturation) flow boiling zone, S_2

The bulk flow boiling zone commences just at the saturation point, see Fig. 3.

Once again, the averaged slip ratio $S_2(z)$ is calculated with the help of the new heat balance

$$h_m(z) = \frac{q}{S_2(z)}(z - z_{sat}) + h_{m,sat} \rightarrow S_2(z) \approx \frac{q(z - z_{sat})}{h_m(z) - h_{m,sat}}. \quad (18)$$

A VOID FRACTION MODEL WITH FIVE PARAMETERS

Figure 4 shows the "measured" slip ratio profile (blue points) derived from the new heat balance, which includes the measured enthalpies (the measured void fraction), following the above procedure of slip averaging by zones.

Clearly, if we were able to predict such slip ratio evolution exclusively from the inlet operating conditions, the new heat balance would not have unknowns, and the mixture enthalpy (thus, the void fraction) could be directly calculated.

Note that there are three discontinuities, namely, at the ONB point where the boiling commences, at the NVG point where the void fraction pace growth increases significantly, and at saturation. As we will comment later, these discontinuities are undertaken by the vapor (the disperse phase). On the other hand, the liquid phase is the continuous phase, and then, the liquid timescale will be the mixture time reference, and, as we will see later, liquid velocity continuity is key for the slip ratio prediction.

In this work, as a first approximation, it is considered that the slip ratio along the partially subcooled flow (ONB–NVG zone) is practically constant. That is,

$$S_0(z) \approx S_{NVG}. \quad (19)$$

Moreover, it has been checked that the slip ratio along the fully subcooled flow is practically linear and a direct function of $S_{1,sat}$; see the slashed red line from z_{sat} to $z = 0$ in Fig. 4; thus,

$$S_1(z) \approx 1 + \frac{S_{1,sat} - 1}{z_{sat}} z. \quad (20)$$

Finally, it was found elsewhere[12] that the constancy of S_2 along saturation supplies good predictions of the void fraction in this zone in spite of the saw tooth profile of $S_2(z)$.

In summary, from the above slip ratio analysis, the following are the five necessary and sufficient parameters to calculate the new slip

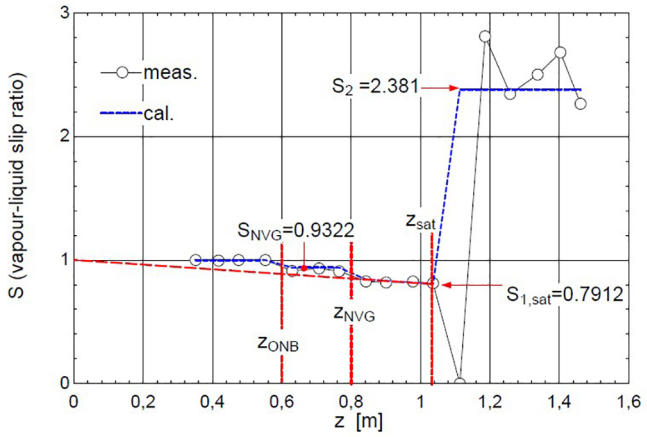

FIG. 4. Slip ratio profile S for tests 1–3.

ratio profile: the location of the ONB (z_{ONB}), the location of the NVG (z_{NVG}), and its void fraction content α_{NVG}, the slip ratio just at saturation, $S_{1,sat}$, and the constant slip ratio along saturation, S_2.

In conclusion, if we were able to find five equations to calculate the above five parameters, which define $S(z)$, we could derive the mixture enthalpy profile from the above new heat balances, Eqs. (13)–(18), and finally to predict the searched void fraction profile from Eqs. (7) and (8).

The following are two brand new relations between $S_{1,sat}$ and S_2, based on fluid kinematics. Assuming as input the other three parameters of the model, these two kinematic equations allow one to calculate the two unknowns, i.e., $S_{1,sat}$ and S_2, then the desired void fraction profile. Figure 2 shows the calculated void fraction, in bold line, using such calculated slips. Regarding z_{ONB}, z_{NVG}, and α_{NVG}, they have been merely varied to best fit the measured void fraction data. Their best fittings values are shown in Fig. 2 for tests 1–3 and also in Table I for all the tests analyzed here.

Continuity of the first derivative of the liquid velocity

As first equation between $S_{1,sat}$ and S_2, it has been suggested the continuity of the first derivative of the mixture specific volume v_m just at saturation, jumping from the subcooled to the bulk flow.

The justification is based on liquid kinematics continuity. Point out that the new mass balance proposed is,[13] see Eq. (10), $Gv_m = u_L$, where G (kg/m^{2}s) is the steady mass flux, and v_m is the mixture specific volume, which is just the inverse of the mixture density

$$v_m = \frac{\alpha\,\rho_G}{\rho_m} v_G + \frac{(1-\alpha)\,\rho_L}{\rho_m} v_L = x v_G + (1-x) v_L. \tag{21}$$

Then, the first derivative continuity of v_m is equivalent to the continuity of the first derivative of the liquid mean velocity, u_L, which is the representative velocity of the mixture. Also note that classic kinematics[15] assumes continuity of motion equations and their derivatives.

Then, the continuity of the first derivative of liquid velocity at saturation is stated as

$$u'_{L1}(z_{sat}) = u'_{L2}(z_{sat}) \;\rightarrow\; v'_{m1}(z_{sat}) = v'_{m2}(z_{sat}), \tag{22}$$

where the prime symbol denotes the first derivative respect to the axial coordinate z, subscript 1 means tending to z_{sat} from subcooling, and subscript 2 denotes tending to saturation point from the bulk zone.

The first derivative of v_m can be related to the new heat balance by means of x, which also appears in h_m, see Eq. (8).

Developing Eq. (21) for the subcooled zone

$$v_{m1} = x v_G + (1-x) v_L \rightarrow v'_{m1} = x'_1 (v_G - v_L) + (1-x) v'_L. \tag{23}$$

Notice that v_L is a function of temperature, i.e., of z, only along the subcooling zone since, in the bulk zone, v_L becomes v_F, the saturated liquid specific volume, with a constant value while the pressure is constant.

Now, the first derivative of x along zone 1 can be readily found from the new heat balance. First, x is cleared from Eq. (8), and then, the first derivative of h_m is performed following Eq. (15)

$$x_1 = \frac{h_m - h_L}{h_G - h_L}, \tag{24}$$

$$x'_1 = \frac{(h'_m - h'_L)(h_G - h_L) + h'_L (h_m - h_L)}{(h_G - h_L)^2} = q \frac{\left(\dfrac{S_1(z) - S'_1 (z - z_{NVG})}{[S_1(z)]^2} - 1 + x \right)}{(h_G - h_L)}, \tag{25}$$

where, from Eq. (12), $h'_L = q$. The first derivative of the subcooling quality evaluated at saturation is

$$x'_1(z_{sat}) = q \frac{\left(\dfrac{S_{1,sat} - S'_1 (z_{sat} - z_{NVG})}{(S_{1,sat})^2} - 1 + x_{sat} \right)}{(h_G - h_F)}. \tag{26}$$

From Eq. (20), $S'_1 = \frac{S_{1,sat} - 1}{z_{sat}}$.

For calculating v'_L, Eq. (23), the volumetric coefficient of thermal expansion β is used, which is classically defined by

$$\beta = -\left(\frac{1}{\rho_L}\right) \frac{d\rho_L}{dT} \text{ (at constant pressure p)}. \tag{27}$$

This volumetric coefficient is supplied in many computer thermodynamic tables. Now, in Eq. (27), the liquid density is substituted by the inverse of the liquid specific volume

$$\beta = \left(\frac{1}{v_L}\right) \frac{dv_L}{dT} \rightarrow \beta v_L = \frac{dv_L}{dz} \frac{1}{\left(\dfrac{dT}{dz}\right)} \rightarrow v'_{L1} = \beta v_L \left(\frac{dT}{dz}\right)_1. \tag{28}$$

Next, for the first derivative of the temperature with respect to the axial coordinate z, we combine the differential form of Eq. (12), and the definition of the liquid specific heat at a constant pressure $c_{p,L}$, function of the liquid temperature, with constant pressure,

$$dh_L = q dz = c_{p,L} dT \;\rightarrow\; \left(\frac{dT}{dz}\right) = \frac{q}{c_{p,L}}. \tag{29}$$

Finally, the first derivative searched and its value at saturation are

$$v'_{L1} = \frac{\beta v_L q}{c_{p,L}} \rightarrow v'_{L1}(z_{sat}) = \frac{\beta(p,\, T_{sat}) v_F q}{c_{p,L(p,\,T_{sat})}}. \tag{30}$$

In conclusion, the first derivative of the mixture specific volume along the fully subcooled boiling zone just at saturation is

$$v'_{m1}(z_{sat}) = q \frac{(v_G - v_F)}{(h_G - h_F)} \left(\frac{S_{1,sat} - S'_1 (z_{sat} - z_{NVG})}{[S_{1,sat}]^2} - 1 + x_{sat} \right) + (1 - x_{sat}) \frac{\beta(p,\, T_{sat}) v_F q}{c_{p,L(p,\,T_{sat})}}. \tag{31}$$

For the derivative of v_m at the bulk zone evaluated at z_{sat} i.e., the right-hand side of Eq. (22), Eq. (21) is stated for the bulk zone

$$v_{m2} = x_2 v_G + (1 - x_2) v_F \rightarrow v'_{m2} = x'_2 (v_G - v_F). \tag{32}$$

The first derivative of x along the bulk zone is found from the heat balance for the bulk flow, Eq. (18). First, the thermodynamic quality is

$$x_2 = \frac{h_m - h_F}{h_G - h_F}. \tag{33}$$

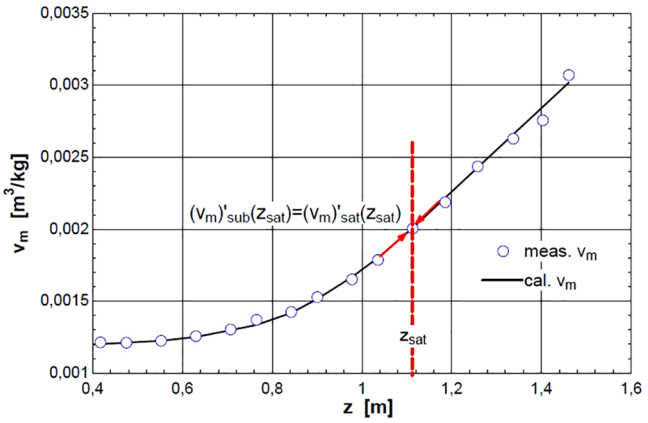

FIG. 5. Calculated v_m profile for tests 1–3.

Then, its derivation is performed, taking into account Eq. (18), evaluated at z_{sat} and included in Eq. (32). Notice that S_2 is assumed constant

$$v'_{m2}(z_{sat}) = \frac{q}{S_2}\frac{(v_G - v_F)}{(h_G - h_F)}. \tag{34}$$

Therefore, the first relation between $S_{1,sat}$ and S_2 is given by equating Eqs. (31)–(34). Figure 5 shows the first derivative continuity of v_m at saturation point crossing from the subcooled to the bulk flow.

Vapor kinematics

The second new equation relates the ONB and S_2 through the vapor velocity profile along bulk flow boiling, see Fig. 6.

First, from the new mass balance, Eq. (10), $u_L(z)$ is easily obtained, provided we have already calculated the mixture specific volume profile, i.e., the void fraction profile.

Now, the vapor velocity profile can be readily obtained from the vapor–liquid velocity ratio, or the slip ratio, definition, Eq. (5). Then, along the saturation zone (subscript 2)

$$u_{G2} = u_{L2}S_2 = Gv_{m2}S_2 \rightarrow u'_{G2} = Gv'_{m2}S_2 = Gq\frac{(v_G - v_F)}{(h_G - h_F)}, \tag{35}$$

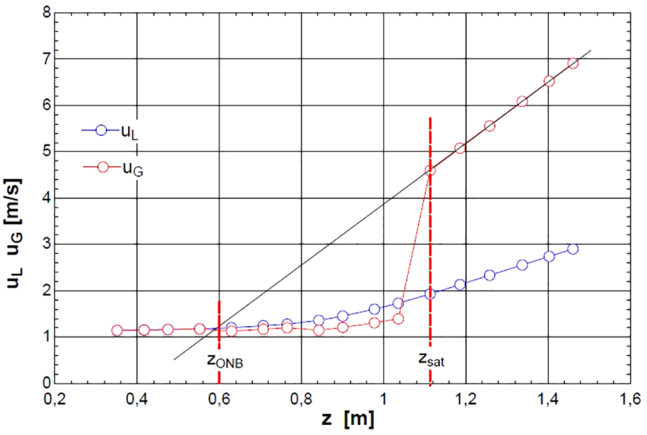

FIG. 6. Calculated u_L and u_G profiles for tests 1–3.

where Eq. (34) has been included. Equation (35) is the slope of the straight line corresponding to the vapor velocity profile along the bulk zone, see Fig. 6.

Finally, as suggested in Fig. 6, the above u_{G2} slope is equated to that of the straight line that connects u_{G2} with the ONB point. Thus,

$$u'_{G2} = Gq\frac{(v_G - v_F)}{(h_G - h_F)} = \frac{u_{G2}(z_{sat}) - u_L(z_{ONB})}{z_{sat} - z_{ONB}} = \frac{S_2 u_L(z_{sat}) - u_L(z_{ONB})}{z_{sat} - z_{ONB}}. \tag{36}$$

RESULTS AND DISCUSSION

Figure 7 shows the modeling of the remaining tests in Table I, which has followed the procedure explained above in detail for tests 1–3.

The agreement is acceptable, but, again, remember that, as a first approximation, three parameters (ONB, NVG, and α_{NVG}), out of the five parameters of the new model, have been varied to best fitting the void fraction data.

Compared with the classic one-dimensional approaches, these three parameters would be reduced to only one, i.e., the equilibrium quality where the NVG point occurs, $x_{e,NVG}$. Remember that the standard void fraction correlations neglect the void fraction content before the NVG point;[1–3] thus, the location of the ONB point is not significant. Moreover, in the standard models, the void fraction curve starts just at the NVG location,[3,5,14] i.e., the void fraction content is zero at NVG. In Fig. 2, this NVG location without vapor content is denoted as z'_{NVG} and has been plotted simply extending backward the fully subcooled void fraction profile until the z axis.

Currently, it is thought that the ability to calculate the NVG point is the most important element in predicting the axial void fraction profile although it is still ongoing in discussion.[16]

Figure 7 can be compared with the results of a very recent work of Niu *et al.*,[17] in which a new model for the 1D transient two-phase two-fluid six-equation model with automatic differentiation approach is presented. In the two-fluid model, two sets of conservation equations describe the balance of mass, momentum, and energy for each phase, as well as the balance equations at the phase interfaces with a large amount of realistic closure correlations.

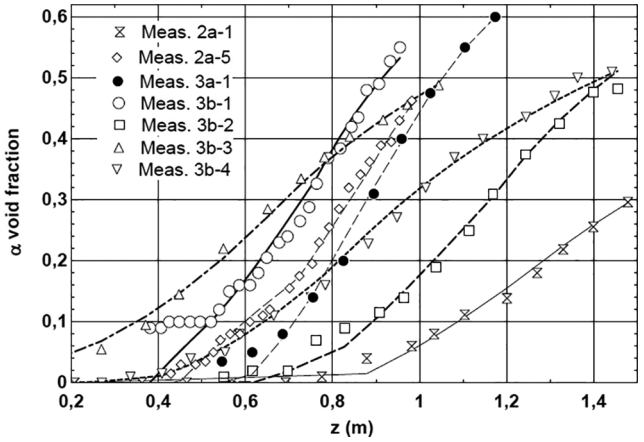

FIG. 7. Measured (points) and calculated (lines) void fraction profiles for Table I tests.

Given the complexity and computing power of the PDE system posed, i.e., it is able to calculate not only the steady but also transient cases, to follow the void fraction as well as pressure drop through a large number of cells along the duct, etc., the number of variables and parameters of the model logically soars. Niu *et al.*[17] validate their model both in the subcooled and saturated flow boiling conditions. For the subcooled experiments, they find good agreement between their model and Bartolomei experimental data.[14] In particular, case 5 in Table 4 in Ref. 17 is test 2a-1 in Table I of this work, and cases 19, 20, and 21 in Ref. 17 coincide with tests 3b-2, 3b-3, and 3b-4 in this work, respectively.

Finally, the slip ratio role as time scaling change factor, see Eq. (11), which is a key point of the new model, is stressed. It has been checked many times[1–4] that phases have different velocities from each other. The key question is if we are considering the same control volume (Euler–Euler treatment) for both phases. Because if the control volume length is the same (the entire duct or some of its sections), their respective timescales should be different from one another too.

In Eq. (9), the time in the heat flux, $q''(\mathrm{kJ/s\,m^2})$, would follow the vapor timescale (bubbles condensing into the subcooled liquid) unlike the time in the inlet liquid mass velocity, $G\,(\mathrm{kg/m^2 s})$, whose reference is obviously that of the liquid time.

In other words, if we combined q'' and G without any time correction, i.e., if we assumed that the phase timescales were the same, we would be considering distinct phase control volumes.

The new heat balance, Eq. (9), is referenced to the liquid timescale, where the liquid is the continuous phase. This is why, in Eq. (9), heat appears divided by the slip ratio, so that both phases be referred to the same timescale (liquid).

Similarly, in the new mass balance, Eq. (10), the vapor mass flow rate appears divided by the slip ratio so that all terms, including time, be referenced to the liquid timescale.

In the same way, applying this time scaling correction to the flow quality concept or mass dryness fraction,[3,4] Eq. (2), this would become identical to the static quality, Eq. (7), used in this work.

CONCLUSIONS

A new one-dimensional void fraction model, based on five parameters, is presented in this work. With the inlet conditions provided (mass flow rate, heat flux, inlet properties, etc.), we should be able to calculate these parameters, which define the slip ratio profile, and thus the mixture enthalpy, from a new heat balance and finally the void fraction.

Also note that, in this work, as a first approach, it is assumed that the model parameters z_{ONB}, z_{NVG}, and α_{NVG} are inputs to the calculation, i.e., they are varied in order to fit the calculated void fraction profile to the measured one. The best fittings for each test are shown in Table I.

However, the brand new two kinematic equations, i.e., Eq. (31) equated to Eq. (34), and Eq. (36), have allowed to calculate the two unknowns, i.e., $S_{1,sat}$ and S_2, and therefore, an acceptable calculated void fraction profile, see Figs. 2 and 7.

In Fig. 3, with a uniform heat flux applied along the tube, the mixture enthalpy, $h_m(z)$, which is exclusively based on operating conditions, void data, and liquid and vapor enthalpies and densities, exhibits a strong change of slope in reaching saturation, which cannot be justified by standard balances. This change of slope, checked many times[9–12] by the author, would justify to explicitly include the mean vapor–liquid velocity ratio, or the slip ratio, $S = u_G/u_L$ dividing to the constant q in the new heat balance in order to follow such slope changes of h_m.

However, note that the slip ratio in the new heat balance was actually included as a timescale conversion factor. Since it has been proposed that heat basically enters the boiling flow through condensing bubbles with the vapor time reference but the common timescale chosen is that of the continuous phase (liquid), so S appears dividing to the heat flux to translate the vapor timescale to the liquid one.

The motion equations[15] would require the continuity of the representative mixture velocity and its derivatives. Since the suggested new mass balance is $G = u_L/v_m$ with G constant, the continuity of the v_m first derivative in Fig. 5 should be equivalent to that of the liquid velocity.

In particular, the continuity of the liquid velocity (mixture volume) first derivative has to be fulfilled at the saturation point, where there is a strong change of the thermodynamic behavior and properties. Therefore, there must be a strong change of the value of the slip ratio, in tests 1–3, from $S_{1,sat} = 0.7897$ to $S_2 = 2.379$, to counteract the thermodynamic changes and, thus, preserve the mixture specific volume first derivative continuity (indeed, liquid velocity first derivative continuity), see Fig. 5.

In conclusion, the suggested justification of the strong change of enthalpy slope profile reaching saturation is to preserve specific volume (liquid velocity) first derivative continuity. Definitely, the enthalpy profile is tightly connected to the mixture specific volume evolution through the slip ratios, which affect to the mixture volume by means of the thermodynamic quality.

At least, the acceptable results about the calculated void fraction, see Figs. 2 and 7, would support this new point of view. Furthermore, the second kinematic condition about the vapor velocity, directly derived from the new mass balance, and which is used in Figs. 2 and 7, would also confirm the new proposals.

Point out that we do not know yet how to calculate the ONB and the NVG points. However, it is thought that the onset of boiling (ONB) could be related to liquid and saturation temperatures of the fluid, and wall temperatures.[18] With regard to the NVG point, it would be relevant a better approach to the slip ratio function along the partially subcooled flow boiling and, again, the application of liquid velocity first derivative continuity at the change between partially and fully boiling flow, which is just the location of the NVG.

Clearly, these preliminary results must be taken with extreme care because not only much more tests have to be analyzed but also the model should be completed.

SUPPLEMENTARY MATERIAL

See the supplementary material (electronic Appendix 1) for a schematic procedure of the void fraction axial profile calculation with the new model and a brief review of the relations between the main parameters is supplied.

AUTHOR DECLARATIONS

Conflict of Interest

The authors have no conflicts to disclose.

Author Contributions

Francisco J Collado: Conceptualization (equal); Data curation (equal); Formal analysis (equal); Investigation (equal); Methodology (equal); Project administration (equal); Resources (equal).

DATA AVAILABILITY

The data that support the findings of this study are openly available at https://www.webofscience.com/wos/woscc/full-record/WOS:A1982PP23000005, Ref. 14.

REFERENCES

[1]J. G. Collier and J. R. Thome, *Convective Boiling and Condensation*, 3rd ed. (Oxford University Press, Oxford, 1994).
[2]A. E. Bergles, J. G. Collier, J. M. Delhaye, G. F. Hewitt, and F. Mayinger, *Two-Phase Flow and Heat Transfer in the Power and Process Industries* (Hemisphere, Washington, 1981).
[3]C. Cai, I. Mudawar, H. Liu, and X. Xi, "Assessment of void fractions models and correlations for subcooled boiling in vertical upflow in a circular tube," Int. J. Heat Mass Transfer **171**, 121060 (2021).
[4]R. T. Lahey, Jr. and F. J. Moody, *The Thermal Hydraulics of a Boiling Water Nuclear Reactor* (American Nuclear Society, La Grange Park, 1979), Chap. 5.
[5]P. Saha and N. Zuber, "Point of net vapour generation and vapour void fraction in subcooled boiling," Int. Heat Transfer Conf. Digital Library **4**, 175–179 (1974).
[6]J. R. S. Thom, "Prediction of pressure drop during forced circulation boiling of water," Int. J. Heat Mass Transfer **7**, 709–724 (1964).
[7]N. Zuber and J. Findlay, "Average volumetric concentration in two-phase flow systems," J. Heat Transfer **87**, 453–468 (1965).
[8]G. E. Dix, "Vapor void fractions for forced convection with subcooled boiling at low flow rates," Ph.D. thesis (University of California, 1971).
[9]F. J. Collado, C. Monne, and A. Pascau, "Changes of enthalpy slope in subcooled flow boiling," Heat Mass Transfer **42**, 437–448 (2006).
[10]F. J. Collado, C. Monne, A. Pascau, D. Fuster, and A. Medrano, "Thermodynamics of void fraction in saturated flow boiling," J. Heat Transfer-Trans. ASME **128**, 611–615 (2006).
[11]F. J. Collado, C. Monne, and A. Pascau, "Void fraction in horizontal blulk flow boiling at high qualities," Energy Convers. Manage. **49**, 644–651 (2008).
[12]F. J. Collado, C. Monne, and A. Pascau, "A new heat balance for flow boiling," AIChE J. **53**, 2123–2130 (2007).
[13]F. J. Collado, "Reynolds transport theorem for a two-phase flow," Appl. Phys. Lett. **90**, 024101 (2007).
[14]G. G. Bartolomei, V. G. Brantov, Y. Molochnikov, Y. Kharitonov, V. A. Solodkii, G. N. Batashova, and V. N. Mikhailov, "An experimental investigation of true volumetric vapour content with subcooled boiling in tubes," Therm. Eng. **29**, 132–135 (1982).
[15]R. Aris, *Vectors, Tensors, and the Basic Equations of Fluid Mechanics* (Dover Publications, Mineola, 1990), Chap. 4.
[16]T. Okawa, "On the mechanism of onset of significant void in subcooled flow boiling," Int. J. Heat Mass Transfer **181**, 121835 (2021).
[17]Y. Niu, Y. He, B. Qiu, F. Xiang, C. Deng, Y. Li, J. Zhang, Y. Wu, W. Tian, G. H. Su, and S. Qiu, "An effective method for modelling 1D two-phase two-fluid six-equation model with automatic differentiation approach," Prog. Nucl. Energy **151**, 104325 (2022).
[18]J. M. Delhaye, F. Maugin, and J. M. Ochterbeck, "Void fraction predicitons in forced convective subcooled boiling of water between 10 and 18 MPa," Int. J. Heat Mass Transfer **47**, 4415–4425 (2004).